Correcting for Model Changes in Statistical Post-Processing – An approach based on Response Theory

Jonathan Demaeyer [1,2] and Stéphane Vannitsem [1,2]

[1]Institut Royal Météorologique de Belgique, Avenue Circulaire, 3, 1180 Brussels, Belgium
[2]European Meteorological Network, Avenue Circulaire, 3, 1180 Brussels, Belgium

Correspondence to: jodemaey@meteo.be

Abstract. For most statistical post-processing schemes used to correct weather forecasts, changes to the forecast model induce a considerable reforcasting effort. We present a new approach based on response theory to cope with slight model change. In this framework, the model change is seen as a perturbation of the original forecast model. The response theory allows then to evaluate the variation induced on the averages involved in the statistical post-processing, provided that the magnitude of this perturbation is not too large. This approach is studied in the context of simple Ornstein-Uhlenbeck models, and then on a more realistic, yet simple, quasi-geostrophic model. The analytical results for the former case allow for posing the problem, while the application to the latter provide a proof-of-concept of the potential performances of response theory in a chaotic system. In both cases, the parameters of the statistical post-processing used – an *Error-in-Variables* Model Output Statistics (EVMOS) – are appropriately corrected when facing a model change. The potential application in a more operational environment is also discussed.

1 Introduction

A generic property of the atmospheric dynamics is its sensivity to initial conditions. This implies that probabilistic forecasts will always be needed to adequately describe this behaviour (Wilks, 2011). Indeed, these methods represent a way to go beyond the natural predictability barrier that the chaotic atmospheric models exhibit (Vannitsem, 2017). These forecasts are at
5 the same time subject to the impact of the presence of structural uncertainties, also known as *model errors*. Such errors degrade the forecasts as well, and their impact needs to be mitigated.

Statistical post-processing methods are used to correct the operational predictions of the atmospheric models. An important family of statistical techniques used to post-process the forecasts are linear regression techniques, with possibly multiple predictors (Glahn and Lowry, 1972; Vannitsem and Nicolis, 2008), also known as Model Output Statistics (MOS). This
10 rather simple but very efficient technique can be adapted to ensemble forecasts (e.g. Vannitsem (2009); Johnson and Bowler (2009); Glahn et al. (2009); Van Schaeybroeck and Vannitsem (2015)). One of the first approaches that was proposed is called *Error-in-Variable* MOS (EVMOS) because it takes into account the presence of errors in the observations and model observables (Vannitsem, 2009).

Despite their simplicity, most post-processing schemes depend on the availability of a database of past forecasts, that allows
15 one to "train" the regression algorithm by comparison with the observations database. These operational models are however subject to frequent evolution cycles, which are needed to improve their representation of the atmospheric behaviours. Therefore, there is a continuous need to recompute past forecasts with the latest model version, to avoid a degradation of the post-processing schemes due to model change. Such recomputation of the past forecasts are called *reforecasts*, and typically requires a huge data storage and management framework, as well as large computational resources (Hamill, 2018). For instance, the
20 *European Center for Medium-range Weather Forecast* (ECMWF) and the *National Weather Service* (NWS) both produce hundreds of reforecasts every week (Hamill et al., 2013).

Recent research have studied non-homogeneous regression with time-adaptative training scheme, where a trade-off have to be considered between large training data sets for stable estimation and the benefit of shorter training periods to adjust more rapidly to changes in the data (Lang et al., 2019). These results can help mitigate the impact of model change on post-processing
25 and may call into question the need for reforecast systems. These systems do however help to better represent rare events, they increase the size of the training data sets and greatly improve sub-seasonal forecasts (Scheuerer and Hamill, 2015; Hamill, 2018), which can justify their prohibitive cost.

The present work investigates another research direction and considers a new technique to reduce the cost of adapting a linear post-processing scheme to a model change. This method relies on the response theory for dynamical systems (Ruelle,
30 2009) and assumes that the model variation can be written as analytical perturbations of the model tendencies. In this context, parameters variations as well as new terms in the tendencies are potential model change.

In section 2, we start by considering simple Ornstein-Uhlenbeck models used to describe the methodology and the concept involved. We show that obtaining a new post-processing scheme after a model change requires the computation of the response of the average of the involved predictors, seen as observables of the system. In the simple case considered, exact analytical re-

sults for the response can be obtained at any order. The correction of the model observables and the post-processing parameters due to the model change only requires the response-theory corrections up to the second order.

In section 3, a more complex case is considered with a toy model of atmospheric variability in the form of a 2-layer quasi-geostrophic model with an orography. We compute the linear response of the predictors of the post-processing for two model change experiments involving a modification of the friction and the horizontal temperature gradient of the model. The response theory approach provides an efficient correction of the post-processing scheme up to a lead time of 3 days, which matches the lead-time window where the scheme's correction is efficient.

In the last section, we discuss the implications that this new method could have on operational forecast post-processing systems, as well as new research avenues to be explored.

2 A simple analytical example

In order to get a first impression of the impact of a model change on a post-processing scheme, we consider two Ornstein-Uhlenbeck processes representing the reality $x(\tau)$ and a model $y(\tau)$ of the reality. These processes obey the following equations:

$$\dot{x} = -\lambda_x\, x + K_x + Q_x\, \xi_x(\tau) \tag{1}$$

$$\dot{y} = -\lambda_y\, y + K_y + Q_y\, \xi_y(\tau) \tag{2}$$

where ξ_x and ξ_y are Gaussian white noise processes such that

$$\langle \xi_x(\tau) \rangle = \langle \xi_y(\tau) \rangle = 0$$

$$\langle \xi_x(\tau)\, \xi_x(\tau') \rangle = \delta(\tau - \tau')$$

$$\langle \xi_y(\tau)\, \xi_y(\tau') \rangle = \delta(\tau - \tau')$$

$$\langle \xi_x(\tau)\, \xi_y(\tau') \rangle = 0$$

These are therefore uncorrelated Ornstein-Uhlenbeck processes with noise amplitudes Q_x and Q_y.

We then consider a change Ψ_y of the model $y(\tau)$, possibly improving or degrading the forecast performances:

$$\dot{\hat{y}} = -\lambda_y\, \hat{y} + K_y + Q_y\, \xi_y(\tau) + \Psi_y(\tau) \tag{3}$$

where

$$\Psi_y(\tau) = -\kappa \left(\delta K + \delta Q\, \xi_y(\tau) \right) \tag{4}$$

with $\delta K = K_y - K_x$ and $\delta Q = Q_y - Q_x$. It can represent, for example, a better parameterisation of subgrid-scale processes or an increase of the model resolution. Note that if $\kappa = 1$, the correction is perfect.

We have thus the reality $x(\tau)$ and two different models of it: $y(\tau)$ and $\hat{y}(\tau)$. We now want to evaluate the difference between a post-processing scheme constructed before the model change (with the past forecasts of the model $y(\tau)$), and one constructed after it (with the past forecasts of model $\hat{y}(\tau)$).

2.1 The post-processing method

5 We now consider a forecast situation where the model y is initialised at the time $\tau = 0$ with a perfect observation of the reality: $y(0) = x(0) = x_0$. We use the *Error-in-Variables Model Output Statistics* (EVMOS) post-processing scheme (Vannitsem, 2009) to correct the forecasts of the model y based on these initial conditions. In this context, given K past forecasts y_k and observations x_k, the correction of the univariate EVMOS post-processing of variable x from a new forecast $y(\tau)$ is provided by the linear regression

$$x_C(\tau) = \alpha(\tau) + \beta(\tau) \cdot y(\tau) \tag{5}$$

The coefficients α and β are obtained by minimising the functional

$$J(\tau) = \sum_{k=1}^{K} \frac{[\{\alpha(\tau) + \beta(\tau) y_k(\tau)\} - x_k(\tau)]}{\sigma_x^2(\tau) + \beta^2(\tau) \sigma_y^2(\tau)} \quad , \tag{6}$$

and are thus given by the equations:

$$\alpha(\tau) = \langle x(\tau) \rangle - \beta(\tau) \langle y(\tau) \rangle \tag{7}$$

$$\beta(\tau) = \sqrt{\frac{\sigma_x^2(\tau)}{\sigma_y^2(\tau)}} \tag{8}$$

where

$$\sigma_x^2(\tau) = \left\langle \left(x(\tau) - \langle x(\tau) \rangle \right)^2 \right\rangle \tag{9}$$

$$\sigma_y^2(\tau) = \left\langle \left(y(\tau) - \langle y(\tau) \rangle \right)^2 \right\rangle \tag{10}$$

The averages $\langle \cdot \rangle$ are taken over an ensemble of past forecasts and observations. This approach has been developed to allow
20 for correct climatological forecast calibration. It constitutes a simple setting in which the impact of model changes can be evaluated and corrected. More sophisticated approaches can be evaluated in the future.

Since we are dealing with simple analytical models here, we can compute the theoretical values of the coefficient α and β with an infinite ensemble of past forecasts, and the averaged quantities involved in this computation are then given by the
25 averages of infinite number of realisations of the Ornstein-Uhlenbeck processes, as if we had an infinite ensemble of past forecasts.

2.2 Averaging the Ornstein-Uhlenbeck processes

For the reality x and the model y, we directly get the averages (Gardiner, 2009)

$$\langle x(\tau) \rangle = \langle x_0 \rangle e^{-\lambda_x \tau} + \frac{K_x}{\lambda_x} \left(1 - e^{-\lambda_x \tau} \right) \tag{11}$$

$$\sigma_x^2(\tau) = \sigma_{x_0}^2 e^{-2\lambda_x \tau} + \frac{Q_x^2}{2\lambda_x} \left(1 - e^{-2\lambda_x \tau} \right) \tag{12}$$

5 and

$$\langle y(\tau) \rangle = \langle x_0 \rangle e^{-\lambda_y \tau} + \frac{K_y}{\lambda_y} \left(1 - e^{-\lambda_y \tau} \right) \tag{13}$$

$$\sigma_y^2(\tau) = \sigma_{x_0}^2 e^{-2\lambda_y \tau} + \frac{Q_y^2}{2\lambda_y} \left(1 - e^{-2\lambda_y \tau} \right) \tag{14}$$

where we note that the model is initialised with the same initial conditions as the reality:

$$\langle y(0) \rangle = \langle x(0) \rangle = \langle x_0 \rangle \qquad , \qquad \sigma_y^2(0) = \sigma_x^2(0) = \sigma_{x_0}^2 \tag{15}$$

10 We get the post-processing coefficients before the model change $\alpha(\tau)$ and $\beta(\tau)$ by inserting these expressions in the equations (7) and (8).

Similarly, we get the same kind of results for the model $\hat{y}$, after the model change Ψ_y:

$$\langle \hat{y}(\tau) \rangle = \langle x_0 \rangle e^{-\lambda_y \tau} + \frac{K_y - \kappa \, \delta K}{\lambda_y} \left(1 - e^{-\lambda_y \tau} \right) \tag{16}$$

$$\sigma_{\hat{y}}^2(\tau) = \sigma_{x_0}^2 e^{-2\lambda_y \tau} + \frac{(Q_y - \kappa \, \delta Q)^2}{2\lambda_y} \left(1 - e^{-2\lambda_y \tau} \right) \tag{17}$$

15 and we also obtain the post-processing coefficients after the model change $\hat{\alpha}(\tau)$ and $\hat{\beta}(\tau)$ (see also the analysis in Vannitsem (2011)). We can also compute the variation of the bias α:

$$\hat{\alpha}(\tau) - \alpha(\tau) = \delta \alpha(\tau) = \beta(\tau) \langle y(\tau) \rangle - \hat{\beta}(\tau) \langle \hat{y}(\tau) \rangle \tag{18}$$

The ratio between the parameters β is given by

$$\frac{\hat{\beta}(\tau)}{\beta(\tau)} = \sqrt{\frac{\sigma_y^2(\tau)}{\sigma_{\hat{y}}^2(\tau)}} \tag{19}$$

20 For $\tau \gg \max(1/\lambda_x, 1/\lambda_y)$, we note that this ratio tends to

$$\frac{\hat{\beta}(\tau)}{\hat{\beta}(\tau)} \approx \frac{1}{1 - \kappa \, \delta Q / Q_y} \tag{20}$$

and the difference between the biases α of the two models is approximatively given by:

$$\delta \alpha(\tau) \approx -\beta(\tau) \frac{K_y}{\lambda_y} \left[\frac{1 - \kappa \, \delta K / K_y}{1 - \kappa \, \delta Q / Q_y} - 1 \right] \quad . \tag{21}$$

Let us now assume that the model change Ψ_y can be considered as a perturbation of the initial model y. Using response
25 theory, the averages $\langle \hat{y} \rangle$ and $\sigma_{\hat{y}}^2$ can be estimated using the initial model y instead of the perturbed model $\hat{y}$. In turn, the use of these new estimated averages allows for computing the new post-processing scheme coefficients $\hat{\alpha}$ and $\hat{\beta}$. We now detail the results obtained by using this method.

2.3 Response theory

After the model change, the forecasts are provided by the model $\hat{y}$ and their time-evolution is given by Eq. (3). This model can be seen as a perturbation of the model y by the term Ψ_y given by Eq. (4). In such case, given an observable A, its average after the model change can then be related to its original average by

$$\langle A(\tau)\rangle_{\hat{y}} = \langle A(\tau)\rangle_y + \delta\langle A(\tau)\rangle_y + \delta^2\langle A(\tau)\rangle_y + \dots \tag{22}$$

where the averages on the right-hand side are taken over the forecasts of model y. Response theory allows to obtain the average over the model $\hat{y}$ forecasts (the left-hand side) based solely on the average over model the y forecasts. The $\hat{y}$ model forecasts are therefore not required to estimate the new post-processing scheme.

The observables depend on the lead time τ of the forecast, as do the parameters α and β which determine the post-processing correction for every lead time. This reflects the fact that the post-processing problem is typically a non-stationary initial value problem, since the initial conditions of the model Eqs. (2) and (3) are typically not chosen on their respective model attractor, but rather as observations[1] of the reality (1). As a consequence, the model averages (22) relax toward the stationary response in the long-time limit, and the stationary response theory (Ruelle, 2009; Wang, 2013) cannot provide us their short-time relaxation behaviour. Instead, the Ruelle time-dependent response theory should be used (Ruelle, 1998a). It follows that, if the perturbation (4) is small, then the first order is given by (see Appendix A):

$$\delta\langle A(\tau)\rangle_y = \int\limits_0^\tau \mathrm{d}\tau' \int \mathrm{d}x_0\, \rho_0(x_0) \left\langle \Psi_y(\tau') \cdot \nabla_{f^{\tau'}(x_0)} A\left(f^\tau(x_0)\right) \right\rangle \tag{23}$$

where ρ_0 is the distribution of the initial conditions (observations) used to initialise the models. ∇_x is the gradient evaluated at the point x, and here it is the simple derivative. As indicated by Eq. (15), in the post-processing framework, it is taken as the stationary/invariant distribution of the reality. It is also assumed that there is no interference due to initial condition errors in the problem. Eq. (23) can be obtained through a Kubo-type perturbative expansion (Lucarini, 2008). We remark that this example deals with stochastic models, due to which we have to perform an additional averaging over the realisations of the stochastic processes, denoted here as $\langle\cdot\rangle$ (Lucarini, 2012). Finally the mapping f^τ which appears in Eq. (23) is the stochastic flow:

$$f^\tau(x_0) = x_0\, e^{-\lambda_y \tau} + \int\limits_0^\tau \mathrm{d}\tau' e^{-\lambda_y(\tau - \tau')} \left[Q_y \xi_y(\tau') + K_y \right]. \tag{24}$$

This maps an initial condition x_0 of the model y to the state $f^\tau(x_0)$ of a realisation of this model at the later lead time τ. The principle of causality is thus implicit in Eq. (23), which estimates the impact of the perturbation Ψ_y on the subsequent perturbed model time-evolution by developing around the unperturbed model y trajectories.

---

[1]Here we consider that the observation are perfectly assimilated in the models, and that there is no observation errors. However in operational setups, such errors are of course to be taken into account.

Evaluating Eq. (23) and its stochastic integrals gives us the variation of the averages $\langle y(\tau) \rangle$ and $\langle y(\tau)^2 \rangle$ to the perturbation Ψ_y:

$$\delta \langle y(\tau) \rangle_y = -\kappa \int_0^\tau \mathrm{d}\tau' \delta K\, e^{-\lambda_y(\tau - \tau')} = -\frac{\kappa}{\lambda_y} \delta K \left(1 - e^{-\lambda_y \tau}\right) \tag{25}$$

$$\delta \langle y(\tau)^2 \rangle_y = -2\kappa \delta K \int_0^\tau \mathrm{d}\tau' \left[\langle x_0 \rangle e^{-\lambda_y(2\tau - \tau')} + \frac{K_y}{\lambda_y} e^{-\lambda_y(\tau - \tau')} \left(1 - e^{-\lambda_y \tau}\right) \right] - 2\kappa \delta Q\, Q_y \int_0^\tau \mathrm{d}\tau'\, e^{-2\lambda_y(\tau - \tau')}$$

$$= -2\kappa \frac{\delta K}{\lambda_y} \langle y(\tau) \rangle \left(1 - e^{-\lambda_y \tau}\right) - \frac{\kappa}{\lambda_y} \delta Q\, Q_y \left(1 - e^{-2\lambda_y \tau}\right) \tag{26}$$

Rearranging these two terms, we also get the following expression for the variation of the variance (14):

$$\delta \sigma_y^2(\tau) = -\frac{\kappa}{\lambda_y} \delta Q\, Q_y \left(1 - e^{-2\lambda_y \tau}\right) - \frac{\kappa^2}{\lambda_y^2} \delta K^2 \left(1 - e^{-\lambda_y \tau}\right)^2 \tag{27}$$

Note that the variation (25) corresponds to the exact difference between the average of the two models $\langle \hat{y}(\tau) \rangle - \langle y(\tau) \rangle$. On the other hand the variation given by Eq. (27) lacks the term of order κ^2 involving δQ that appears in the exact difference $\sigma_{\hat{y}}^2(\tau) - \sigma_y^2(\tau)$ given by Eqs. (14) and (17). Instead, another term of order κ^2 and involving δK is present, indicating that we need to consider the higher-order term of response theory Ruelle (1998b) to correct it. The second-order term is given by the expression (Lucarini, 2012):

$$\delta^2 \langle A(\tau) \rangle_y = \int_0^\tau \mathrm{d}\tau' \int_{\tau'}^\tau \mathrm{d}\tau'' \int \mathrm{d}y\, \rho_0(x_0) \left\langle \Psi_y(\tau') \cdot \nabla_{f^{\tau'}(x_0)} \Psi_y(\tau'') \cdot \nabla_{f^{\tau''}(x_0)} A\left(f^\tau(x_0)\right) \right\rangle. \tag{28}$$

Applying this to the first moment of the y models directly yields

$$\delta^2 \langle y(\tau) \rangle_y = 0. \tag{29}$$

On the other hand, integrating the stochastic integrals present in this expression for the moment $\langle y(\tau)^2 \rangle$ gives

$$\delta^2 \langle y(\tau)^2 \rangle_y = \frac{\kappa^2\, \delta K^2}{\lambda_y^2} \left(1 - e^{-\lambda_y \tau}\right)^2 + \frac{\kappa^2\, \delta Q^2}{2\lambda_y} \left(1 - e^{-2\lambda_y \tau}\right) \tag{30}$$

which corrects the $\kappa^2 \delta K^2$ term in Eq. (27) and makes the response theory up to order 2 exactly match the difference $\sigma_{\hat{y}}^2(\tau) - \sigma_y^2(\tau)$, for every lead time τ. In fact, the subsequent orders of the response vanish due to the linearity of the simple Ornstein-Uhlenbeck models, which allows to truncate the response Kubo-like expansion to the second order. Finally, this shows that the (non-stationary) response theory can be used to estimate the post-processing parameters after the model change based on the forecasts of the initial model. Indeed, instead of the averages $\langle \hat{y}(\tau) \rangle$ and $\langle \sigma_{\hat{y}}^2(\tau) \rangle$, the approximate averages $\langle y(\tau) \rangle + \delta \langle y(\tau) \rangle_y$ and $\sigma_y^2(\tau) + \delta \langle \sigma_y^2(\tau) \rangle_y + \delta^2 \langle \sigma_y^2(\tau) \rangle$ can be used to compute $\hat{\alpha}$ and $\hat{\beta}$. We emphasise that the second order contribution had to be considered in order to obtain the exact result. Nevertheless, the difference between the first and the second order response is of order κ^2, which implies that for a small perturbation (model change), the first order will generally be a sufficiently good approximation. A more detailed derivation of the results obtained in this section can be found in the supplementary material.

In order to investigate this research avenue on a case closer to those encountered in reality, we will now consider the application of post-processing and response theory to a low-order atmospheric model displaying chaos.

3   Application to a low-order atmospheric model

A 2-layer quasi-geostrophic atmospheric system on a β-plane with an orography is considered (Charney and Straus, 1980; Reinhold and Pierrehumbert, 1982). This spectral model possesses well-identified large-scale flow regimes, such as *zonal* and *blocked* regimes. The horizontal adimensionalised coordinates are denoted x and y. The two main fields of this model are the

5   500 hPa pressure anomaly and temperature, which are proportional to the barotropic streamfunction $\psi(x,y)$ and the baroclinic streamfunction $\theta(x,y)$, respectively. These fields are expanded in Fourier modes:

$$
\begin{aligned}
F_1(x,y) &= \sqrt{2}\cos(y), \\
F_2(x,y) &= 2\cos(nx)\sin(y), \\
F_3(x,y) &= 2\sin(nx)\sin(y), \\
F_4(x,y) &= \sqrt{2}\cos(2y), \\
&\vdots
\end{aligned}
$$

such that

$$
\nabla^2 F_i(x,y) = -a_i^2 F_i(x,y) \tag{31}
$$

with eigenvalues $a_1^2 = 1$, $a_2^2 = a_3^2 = 1 + n^2$, $a_4^2 = 4, \ldots$, where n is the aspect ratio of the x-y domain. We have thus the

15   following decomposition

$$
\psi(x,y) = \sum_{i=1}^{n_{\mathrm{a}}} \psi_i\, F_i(x,y) \tag{32}
$$

$$
\theta(x,y) = \sum_{i=1}^{n_{\mathrm{a}}} \theta_i\, F_i(x,y)\quad. \tag{33}
$$

where n_{a} is the number of modes of the spectral expansion. The partial differential equations controlling the time evolution of the fields $\psi(x,y)$ and $\theta(x,y)$ can then be projected on the Fourier modes to finally give a set of ordinary differential equations

20   for the coefficients ψ_i and θ_i:

$$
\dot{\boldsymbol{x}} = \boldsymbol{F}(\boldsymbol{x}) \quad, \quad \boldsymbol{x} = (\psi_1, \ldots, \psi_{n_{\mathrm{a}}}, \theta_1, \ldots, \theta_{n_{\mathrm{a}}}) \tag{34}
$$

that can be solved with usual numerical integrators. All variables are adimensionalized.

In the version proposed by Reinhold and Pierrehumbert using the 10 first modes, beyond a certain value of the zonal temperature gradient, the system displays chaos and makes transitions between the blocked and zonal flow regimes embedded in

25   its global attractor. Here, we adopt their notations and main adimensionalized parameters values: the friction at the interface between the two layers $k = 0.05$, the friction at the bottom surface $k' = 0.01$, and the aspect ratio of the domain $n = 1.3$. The β-plane lies at mid-latitude (45°) and the Coriolis parameter f_0 is set accordingly.

In the present work, the parameter h, the Newtonian cooling coefficient is fixed to 0.1 instead of the value found in Reinhold and Pierrehumbert (which is $h = 0.045$). Two additional fields have to be specified on the domain: $\theta^\star(x,y)$, the radiative
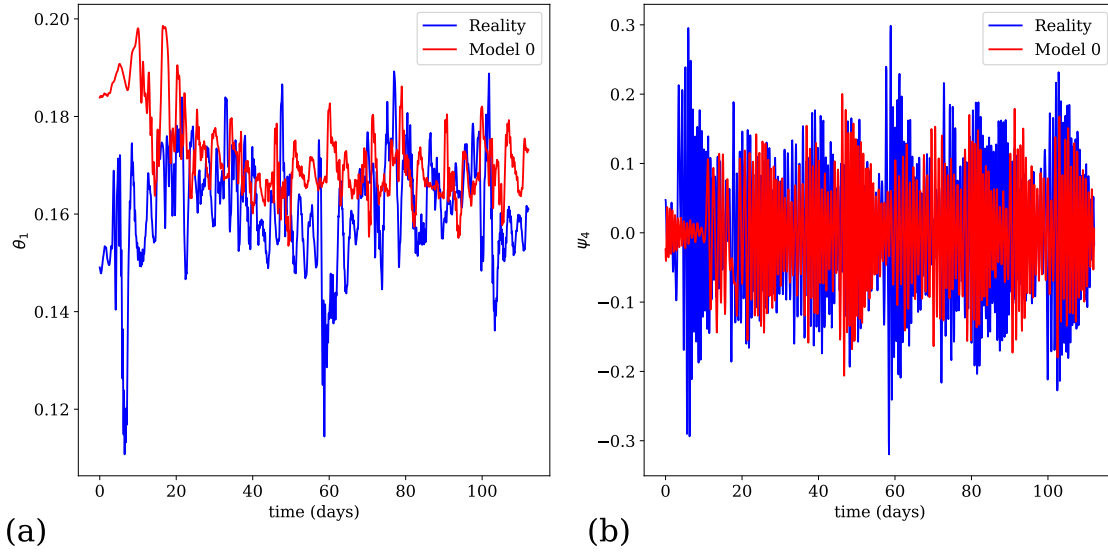
Figure 1. Dynamics of reference system and model 0 of the post-processing experiment with change of friction (see Table 1), for: (a) time evolution of the variable θ_1, (b) time evolution of the variable ψ_4.

equilibrium temperature field, and $\hbar(x, y)$, the topographic height field. These fields can be decomposed by projecting them onto the eigenfunctions of the Laplacian as before. The corresponding coefficients $\theta_i^\star$ and $\hbar_i$ then allow for writing these fields as sums of weighted eigenfunctions:

$$\theta^\star(x,y) \quad = \quad \sum_{i=1}^{n_a} \theta_i^\star \, F_i(x,y) \tag{35}$$

$$5 \quad \hbar(x,y) \quad = \quad \sum_{i=1}^{n_a} \hbar_i \, F_i(x,y) \quad . \tag{36}$$

In the present case, we consider that the only non-zero coefficients are $\theta_1^\star = 0.2$ and $\hbar_2 = 0.2$, meaning that the radiative equilibrium profile is given by the zonally varying function $\sqrt{2}\cos(y)$ and the orography is made of a mountain and a valley shaped by the function $2\cos(nx)\sin(y)$. Again, the value of the temperature gradient $\theta_1^\star$ is larger than the one chosen in Reinhold and Pierrehumbert (which is $\theta_1^\star = 0.1$) to increase the chaotic variability in the system. Trajectories of variables θ_1 and ψ_4 are

10 depicted in Fig. 1, for the reference system (reality) and a model version (model 0) for which the friction coefficient has been slightly modified.

These parameter changes induce slight modifications of the dynamics. In particular the system possesses two distinct weather regimes, depicted in Fig. 2(b): one characterised by a zonal circulation (see Fig. 1(c)), and another characterised by a blocking situation (see Fig. 1(d)). This is different from the case considered in Reinhold and Pierrehumbert (1982), where two blocking

15 regimes coexist with the zonal regime.

(a)

(b)

(c)

(d)
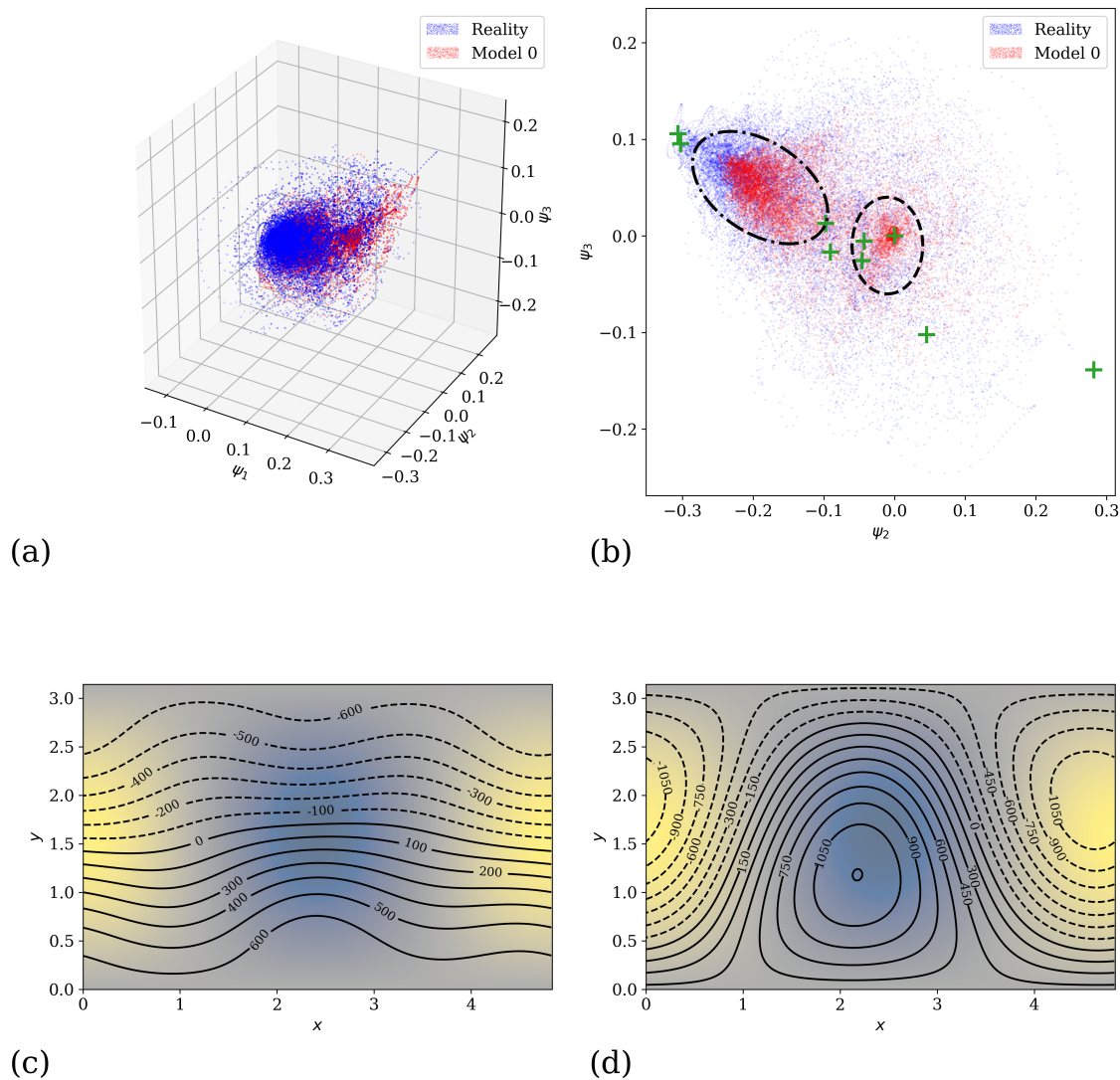
Figure 2. (a) 3D scatter plot of the attractors along the variables ψ_1, ψ_2 and ψ_3, (b) 2D scatter plot of the attractors along the variables ψ_2 and ψ_3. Two different parts of the attractors are indicated by ellipses. The green crosses correspond to equilibrium points of the reference model, the reality. The dashed ellipse corresponds on average to a zonal circulation depicted on panel (c). The dashed-dotted ellipse corresponds on average to a blocking situation depicted in panel (d). In both panels (c) and (d), the underlying colour map denotes the orography on the domain, and the contours the geopotential height anomaly at 500 hPa.

Parameter description / Experiment	Symbol / System	Reality	Newtonian cooling modification		Friction coefficient modification	
			Model 0	Model 1	Model 0	Model 1
Newtonian cooling coefficient	h	0.1	0.102	0.101	0.1	
Atm. layers friction	k	0.05	0.05		0.06	0.055
Bottom layer friction	k'	0.01				
Domain aspect ratio	n	1.3				
Meridional temperature gradient	$\theta_2^\star$	0.2				
Mountain ridge altitude	h_2	0.2				

Table 1. The main parameters used and modified in the experiments. Model 0 and model 1 are respectively the forecast model of the reality before and after the model change.

3.1 Post-processing experiments

The model described above with 10 modes ($n_\mathrm{a} = 10$) is used and two different post-processing experiments are performed, one involving the Newtonian cooling parameter h and another involving the friction parameter k between the two atmospheric layers. The parameter values detailed above correspond to the long-term reference (i.e. the reality). A first model is defined (model 0) which is a copy of the 2-layer quasi-geostrophic model defining the reality, but the parameters h or k are slightly changed, i.e. the model error of the forecasting system lies in either the Newtonian cooling or the friction parameter. Then, as in Section 2, a model change is imposed, leading to another forecasting model (model 1) that can either improve or degrade the model error by a factor κ. The parameter variations involved in these experiments are detailed in Table 1. Without loss of generality, we consider model changes that improve the representation of reality, in the sense that the amplitude of the model errors in model 1 is smaller than in model 0. The effect of the model change is depicted in Figs. 3 and 4 for the friction parameter experiment. These figures display the mean and the standard deviation of the model forecasts and observations coming from the reference forecasts, as a function of the lead time τ. We have used a set of one million trajectories of each system to compute these averages.

In the framework of the EVMOS post-processing scheme, the predictors and the predictands are the same nominal variable and no other predictors are used. In both experiments considered, the post-processing parameters α and β of the EVMOS for model 0, as well as $\hat{\alpha}$ and $\hat{\beta}$ for model 1, are computed. The main objective here is then to estimate the difference between the former and the latter using Ruelle response theory. The approach in a multivariate setting is presented below.

3.2 Response theory and the tangent linear model

Let us consider again the response theory described in Section 2.3, but in the multivariate deterministic case. In the post-processing framework, models 0 and 1 evolve in time from a set of initial conditions taken outside of their respective attractors. Response formulae found in Ruelle's work have to be adapted to take this into account. One therefore has to consider the
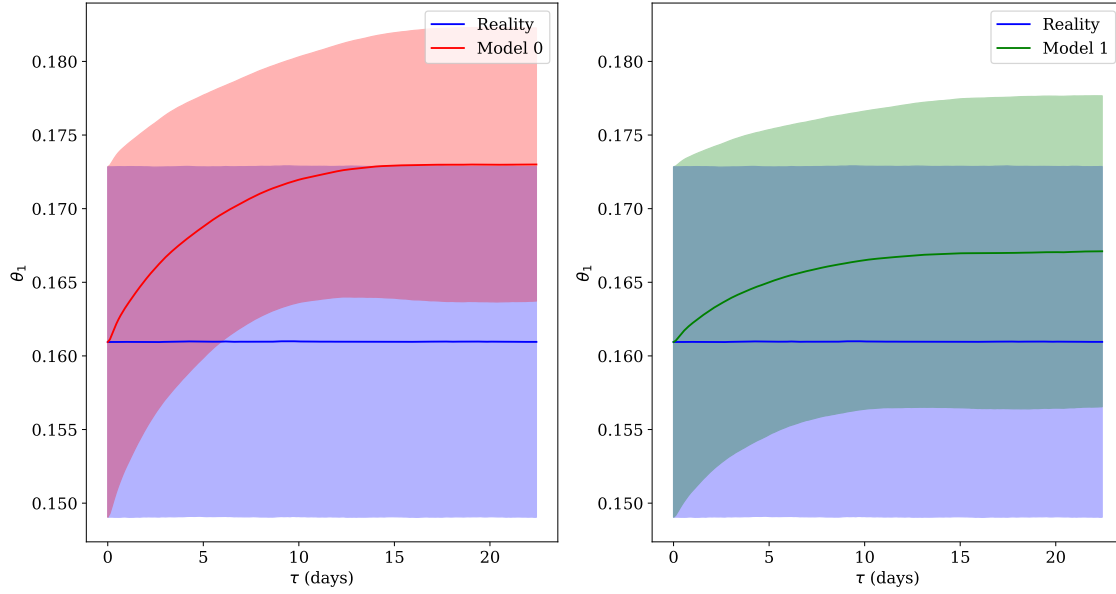
Figure 3. Behaviour of the averages as a function of the lead time τ in the reality and the forecast models before (left panel) and after (right panel) the model change, in the case of the friction post-processing experiment (see Table 1). The variable considered is the temperature meridional gradient θ_1. The solid lines denote the mean while the shaded areas denote the one standard deviation interval.

density of initial conditions as the measure. For a system with a time-independent perturbation $\boldsymbol{\Psi}(\hat{\boldsymbol{y}})$,

$$\dot{\hat{\boldsymbol{y}}} = \boldsymbol{F}(\hat{\boldsymbol{y}}) + \boldsymbol{\Psi}(\hat{\boldsymbol{y}}) = \hat{\boldsymbol{F}}(\hat{\boldsymbol{y}}), \tag{37}$$

an observable A with average $\langle A(\tau)\rangle_{\boldsymbol{y}}$ at the lead time τ for the system

$$\dot{\boldsymbol{y}} = \boldsymbol{F}(\boldsymbol{y}) \tag{38}$$

5   has a first order response of

$$\delta\langle A(\tau)\rangle_{\boldsymbol{y}} = \int \mathrm{d}\boldsymbol{y}_0 \, \rho_0(\boldsymbol{y}_0) \, \boldsymbol{\delta y}(\tau)^{\mathsf{T}} \cdot \boldsymbol{\nabla}_{\boldsymbol{f}^{\tau}(\boldsymbol{y}_0)} A \tag{39}$$

where $\boldsymbol{f}^{\tau}$ is the flow of the unperturbed system (38), ρ_0 is the distribution of initial conditions, and $\boldsymbol{\delta y}(\tau)$ is the solution of the equation $\dot{\boldsymbol{y}} + \dot{\boldsymbol{\delta y}} = \hat{\boldsymbol{F}}(\boldsymbol{y} + \boldsymbol{\delta y})$ which can be approximated at first order by the following linear inhomogeneous differential equation

10   $$\dot{\boldsymbol{\delta y}} = \boldsymbol{\nabla}_{\boldsymbol{y}} \boldsymbol{F} \cdot \boldsymbol{\delta y} + \boldsymbol{\Psi}(\boldsymbol{y}). \tag{40}$$
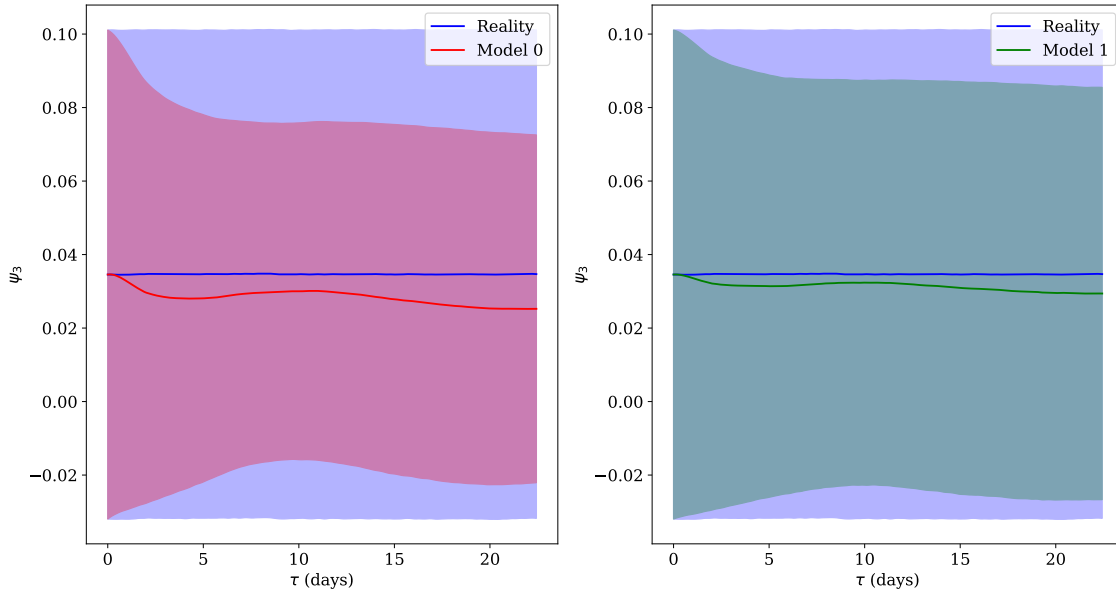
Figure 4. Same as Figure 3, but for the variable ψ_3 of the streamfunction ψ.

where $\boldsymbol{y}(\tau)$ is solution of the unperturbed equation (38) with initial condition $\boldsymbol{y}(0) = \boldsymbol{y}_0$ and we see that the systems (38) and (40) have to be integrated simultaneously (Gaspard, 2005). The homogeneous part of Eq. (40) is the well-known tangent linear model of the system and here it has to be solved with an additional boundary term which is the perturbation itself.

Equation (39) is derived in Appendix A, and can be computed in the same way as the averages depicted in Figs. 3 and 4,

5   by averaging over multiple initial conditions of the reference system. Since we initialise the unperturbed (model 0) and the perturbed systems (model 1) with the same initial conditions, the initial state of the tangent model (40) is $\boldsymbol{\delta y}(0) = 0$. Therefore we do not estimate the impact of the observation or assimilation errors, but rather the direct impact of the model errors viewed as time-independent perturbations. The formulation of the problem and Eq. (40) can be adapted to take these errors into account, as described for instance by Nicolis (2016).

10   In what follows, we will numerically integrate Eq. (40) to evaluate the response on the average due to the perturbation induced by the model change. This will in turn, as in Section 2, allow us to compute the post-processing parameters for the new model.

3.3   Main results

For each of the two experiments detailed in Table 1, we start by obtaining one million observations of the reality that will

15   be used to initialise the forecast models. For each observation, this is done by starting the model $\boldsymbol{x}$ (the reference) with a

random initial condition and running it for a very long time (100000 adimensionalized time units) to achieve convergence to its global attractor. Once the observations have been obtained, we run the reference model, model 0 and model 1 over 200 time units (corresponding to roughly 22 days) to obtain the reality and the forecasts. The systems have been integrated using the fourth-order Runge-Kutta integration scheme with a time-step of 0.1 time unit corresponding to 16.15 minutes. The averaging

5   over the one million trajectories of the reality and of the forecasts at each lead time allow for computing the post-processing coefficients α and β of the EVMOS by using formulas (7) and (8). For each variable, the variable itself is used as the unique predictor.

The response-theory approximations of the averages of the model $\hat{y}$ (model 1) averages are obtained by integrating the linearised equations of model 0 along its trajectories with the perturbation $\boldsymbol{\Psi}$ as inhomogeneous term. This is done by integrating

10 Eq. (40) over a lead time of 200 time unit with a zero initial condition, using the same integration scheme as before. It allows us to obtain the integrand of Eq. (39) for each trajectory, and the integral is then approximated as the average of this integrand over the whole set of trajectories. The result of this integration and averaging is shown in Figs. 5 and 7 for the first and second moment of the variable θ_1. The results for other variables are available in the supplementary material. The black curve shows the moments of model 0 with the addition of their linear response $\delta\langle\theta_1\rangle$ and $\delta\langle\theta_1^2\rangle$ to the perturbation Ψ. This curve agrees

15 well with the green curves of the model 1 moments up to a lead time of 3 or 4 days, showing the efficiency of response theory. Note that in contrast with the calculation of the averages shown in Figs. 3 and 4 and computed with one million trajectories, we have here considered a limited subset of 10000 trajectories of model 0 and its tangent to compute the corrections to these averages. The correction of the moments of model 1 are accurate until 3 days for both experiments. After this critical lead time, obtaining a good accuracy requires a huge increase in the number of forecasts and tangent model integrations to perform

20 the averaging. This problem is well-known (Nicolis, 2003; Eyink et al., 2004) and is due to the appearance of fat-tails in the distribution of the perturbations $\boldsymbol{\delta y}$ in the integrand of Eq. (39). As it can be seen in Fig. 9, the problem worsens with the increase of the lead time: initially the distributions are near-Gaussian and fat-tails appears progressively. Therefore, the number of samples of $\boldsymbol{\delta y}$ needed to converge to the correct mean up to a certain precision increases exponentially as the lead time increases. This problem has consequences on the method used to perform the average. Indeed, to avoid rare and unrealistic

25 extreme response of the system located far in the tails of the distributions, we have removed outliers above a certain threshold (set to 3. adimensional unit) from the averaging.

The moments obtained by the response theory approach are used to compute new EVMOS post-processing α and β coefficients, thanks to the formulas (7) and (8). In Figs. 6 and 8, we compare the three post-processing schemes hence obtained: the post-processing of model 0 (red curves) and 1 (green curves) obtained by averaging over their trajectories (forecasts), and

30 the post-processing of model 1 obtained with the response theory approach (black crosses). In the panel (a) of these figures, the mean square error (MSE) between the trajectories of the models and the reference trajectories is displayed by solid curves, while the MSE between both models correction and the reference is depicted by dash-dotted curves. In general, the corrections are efficient until a lead time of 3-4 days. In fact, the skill of the corrections decreases with the lead time, and thus the EVMOS schemes become not better than the original models after 3 days. In the panels (b) and (c) of Figs. 6 and 8, the mean and

35 variance of the corrected forecasts is compared with those of the original models. Again, these corrections are efficient until
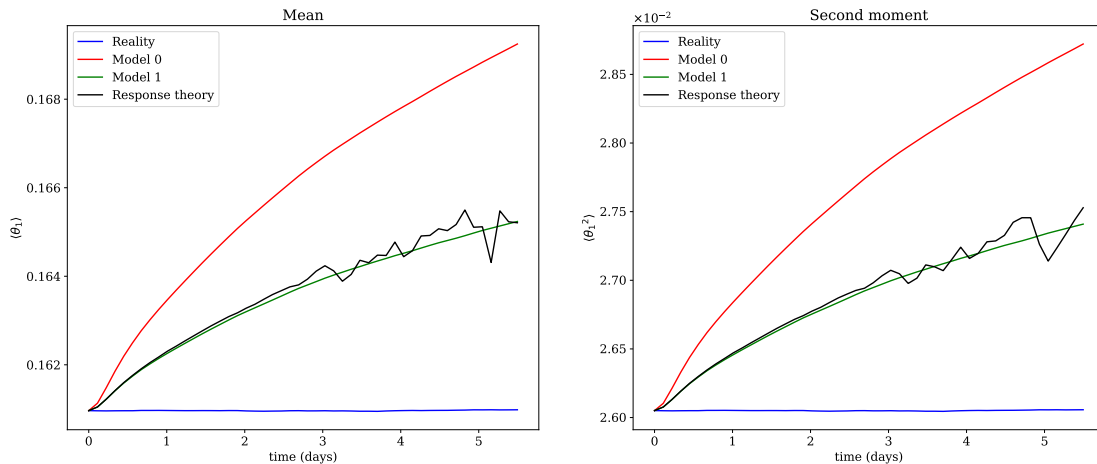
Figure 5. Corrections of the moments of θ_1 from model 0 to model 1 using the response theory formula (39), for the experiment with varying friction coefficient.

3 days for all the post-processing scheme considered. For all the 3 panels of these figures, the correction of model 1 using the response-theory EVMOS is depicted by black crosses and it matches almost perfectly the score of the "exact" EVMOS obtained with the forecasts of model 1 (dash-dotted green curve), up to a 3 days lead time. After that lead time, the errors due to the fat-tails in the response of the first moments of the statistics induce errors in the variance needed to compute the α and β

5   coefficients (see Eqs. (7) and (8)). These coefficients therefore degrade sharply after 3 days, as shown by the solid black curve in Fig. 10 (c) and (d). This in turn induces a degradation of the response theory post-processing scheme, as depicted in Figs. 6 and 8.

Nevertheless, this limitation of response theory is not a concern for our present aim, since after the critical lead time of 3 days, the EVMOS skill vanishes anyway. In conclusion, obtaining accurate EVMOS coefficients is therefore critical up to 3

10   days, which is precisely the timespan where the response theory is the most accurate.

4   Discussion and Conclusions

Statistical post-processing techniques used to correct numerical weather predictions (NWP) require substantial past forecast and observation databases. In the case of a model change, which frequently occurs during the normal life cycle of an operational forecast model, one has to reforecast the entire database of past forecasts (Hagedorn et al., 2008; Hamill et al., 2008) to update

15   the post-processing coefficients and parameters. In the present work, we proposed a new methodology based on response theory to produce these new coefficients without having to reforecast. Instead, the database of past forecasts is reused to perform integrations in the tangent space of the model. It allows to obtain the new post-processing coefficients as modifications of the

(a)

(b)

(c)
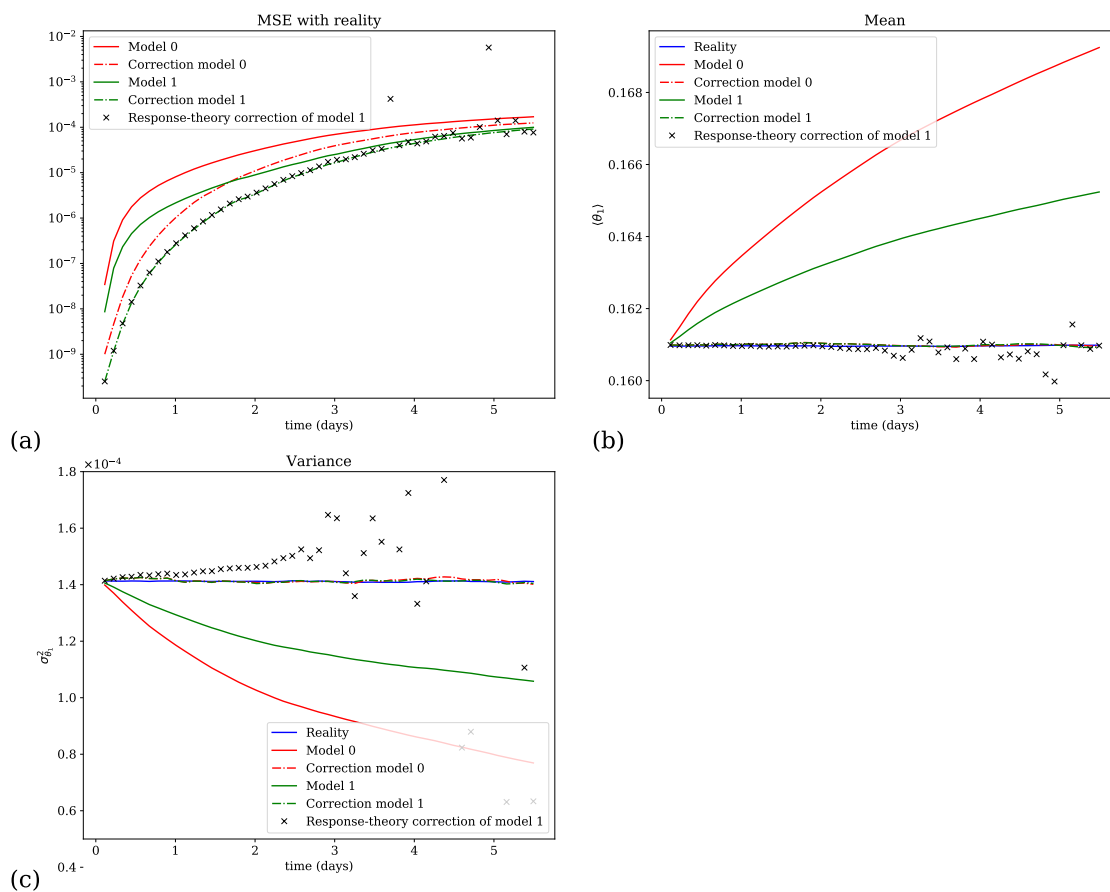
Figure 6. Performance of the corrections on the variable θ_1 for the experiment varying the friction coefficient. (a) Mean square error (MSE) evolution between the different forecasts and their correction, and the reality. (b) Mean of the different trajectories (reality, model 0 and 1) and corrected forecasts. (c) Variance of the different trajectories and corrected forecasts.
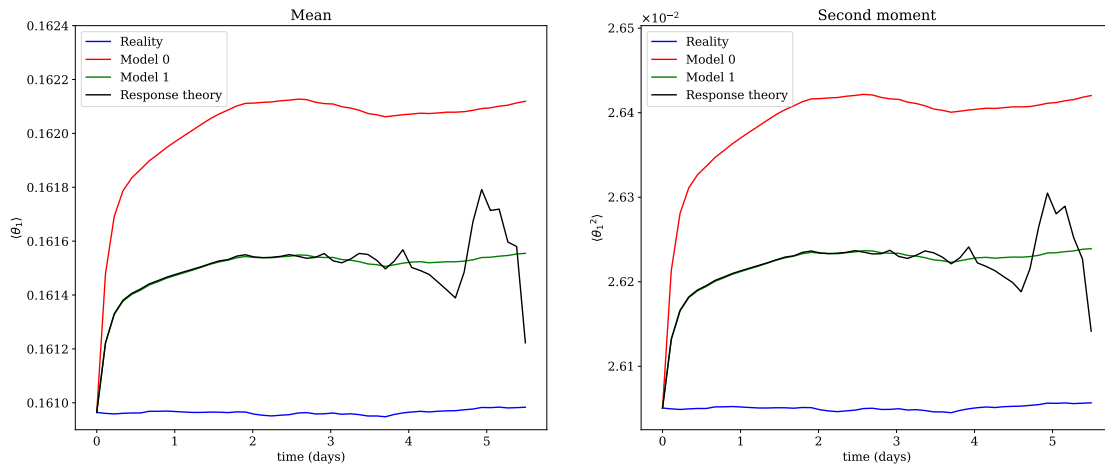
Figure 7. Corrections of the moments of θ_1 from model 0 to model 1 using the response theory formula (39), for the experiment with varying Newtonian cooling coefficient.

older ones. These new coefficients were shown to be accurate enough within the lead time range for which the post-processing corrections improve the forecast.

Figure 10 summarises the main results of this work, with the quasi-geostrophic system described in Section 3, but using a different number m of trajectories of model 0 and its tangent model to compute the response-theory corrections. It shows that 5   up to a lead time of 2 days, good post-processing scheme coefficients are obtained even with a mere 20 integrations in the tangent space.

Note however that in the context of this conceptual quasi-geostrophic model, it turns out one can also obtain good estimates of the post-processing coefficients α and β simply by using a small set of reforecasts. For this it suffices to directly integrate the updated model 1, given by the non-linear equation (37), for only 20 trajectories. So the response theory approach in the present 10   case cannot really compete with the simple reforcasting method. How this can be improved in an operational context is an important question that should be addressed in the future. For instance, we can use a simplified tangent linear model to reduce the computational burden, as often used in data assimilation (Bonavita et al., 2017). This approach could also be implemented for short-range forecasts, say from 1 to 3 days.

The response-theory is efficient because the model changes are assumed to be small in comparison with the original pa-15   rameterisation of the models. The method cannot improve a post-processing scheme, but it can efficiently adapt it to a new model. As such, the success of this method also depends on the quality of the past post-processing scheme. There are also situations where linear response theory is known to fail, but statistical tests which allow to identify its breakdown have been derived in Gottwald et al. (2016) and in Wormell and Gottwald (2018). In addition, the approach presented here applies only
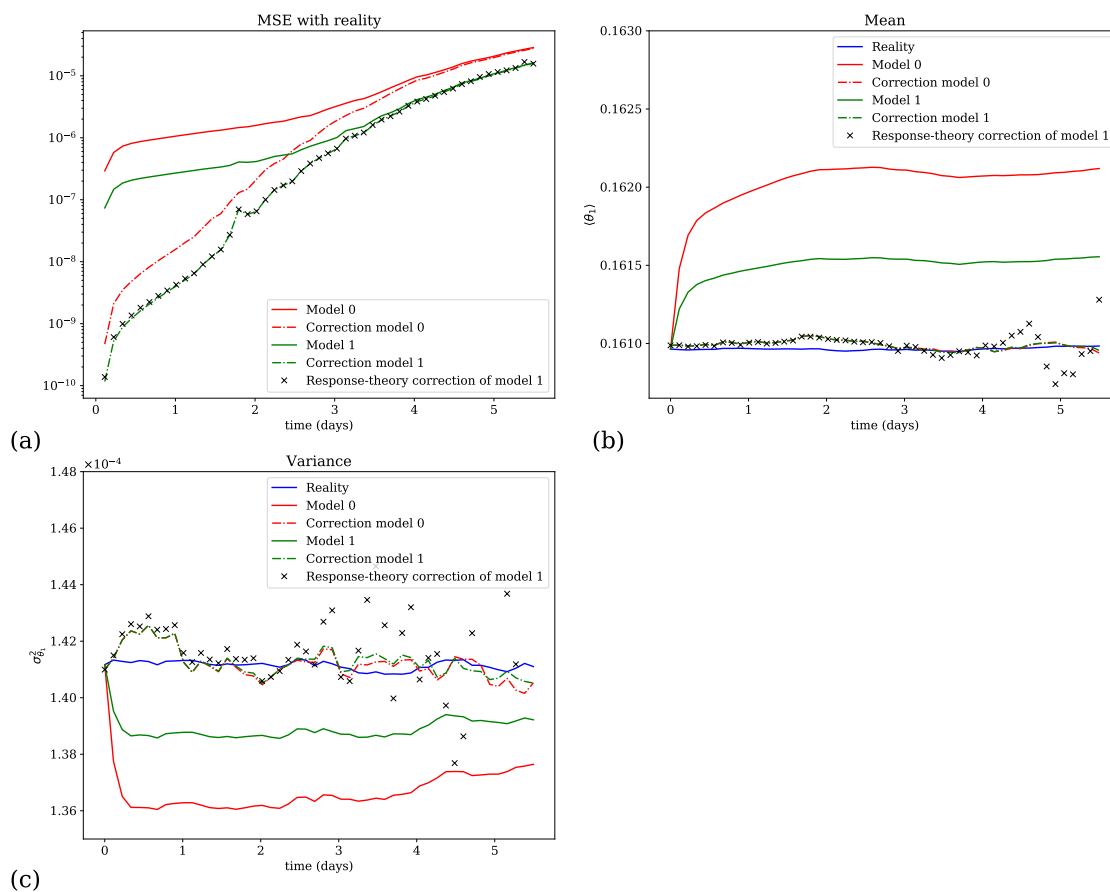
Figure 8. Performance of the corrections on the variable θ_1 for the experiment varying the Newtonian cooling coefficient. (a) Mean square error (MSE) evolution between the different forecasts and their correction, and the reality. (b) Mean of the different trajectories (reality, model 0 and 1) and corrected forecasts. (c) Variance of the different trajectories and corrected forecasts.
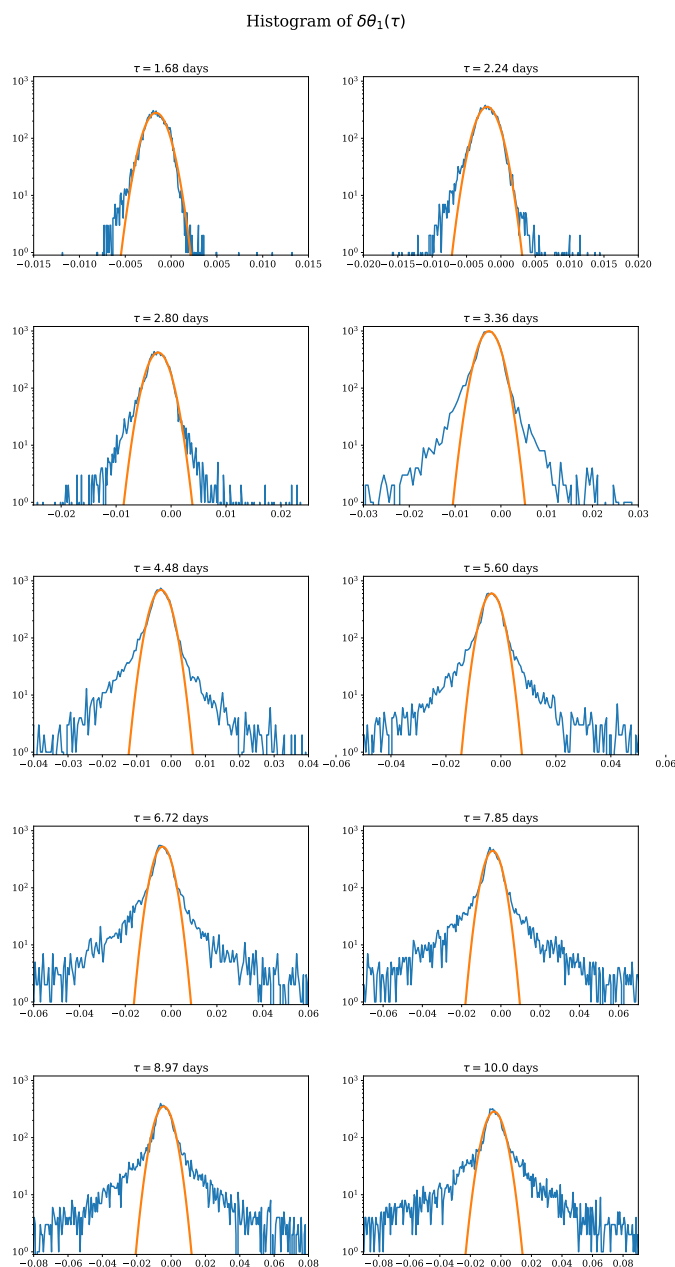
Figure 9. Histograms of the solutions of the equation (40) for the perturbation $\delta y(\tau)$ along the trajectories of model 0, for different values of the lead time τ. The solid orange curves are fits of a Gaussian distribution function to the different histograms. The fat-tail phenomenon described in Eyink et al. (2004) is apparent and becomes more prominent as the lead time increases.
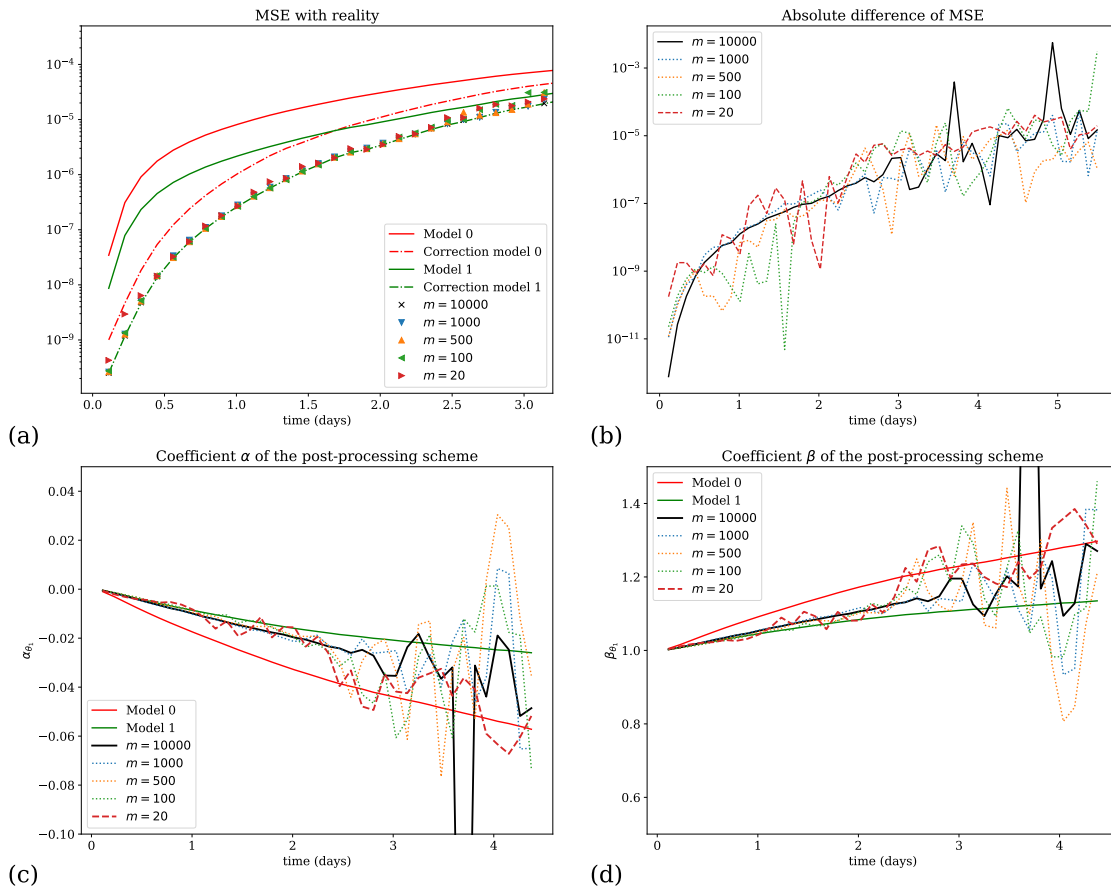
Figure 10. Comparison of the efficiency of the response theory correction for different numbers m of trajectories used to average Eq. (39), for the experiment of varying the friction coefficient: (a) Mean square error with reality, (b) Absolute difference between the response theory correction and the correction based on the forecast of model 1, (c) and (d) Post-processing coefficients α and β. On the panels (b), (c) and (d), the higher (100000) and the lower (20) numbers are depicted respectively by a solid black line and a dashed red line. The other cases in-between are depicted by dotted lines.

for models for which a tangent model is available. The model change itself has to be provided as an analytic function, which can in some circumstances limit of the applicability of the approach.

To test this approach, we have focused on the EVMOS statistical post-processing method, but other methods could be considered as well. The only requirement is that the outcome of the minimisation of the cost functions uses averages of the systems being considered. In fact, we hypothesise that any statistical method using average quantities could be concerned by our approach. For instance, member-by-member methods that correct both the mean square errors and the spread of the ensemble while preserving the spatial correlation (Van Schaeybroeck and Vannitsem, 2015) could be considered. These methods generally use the covariance between the model forecasts and the observations as ingredient, instead of their marginal variance for the EVMOS. However, it does not preclude the applicability of response theory since this covariance can easily be written as an ensemble average. This will be investigated in a future work, together with the applicability of the approach to parameters of probability distributions, as often used in meteorology (Vannitsem et al., 2018).

The impact of initial condition errors has not been addressed here, since the purpose was to demonstrate the applicability of the approach in a perfectly controlled environment. The main limiting issue of response theory in the present context is the presence of fat tails in the distribution of the perturbations δy in the tangent model. This implies that beyond a certain lead time, typically 2-3 days for the synoptic scale, the number of trajectories of the tangent model needed for the averages to converge increases exponentially. This renders the approach impractical at lead times beyond 2-3 days. This is a well-known problem, which is typically due to the trajectories passing close to the stable manifolds structuring the dynamics of chaotic systems (Eyink et al., 2004), generating an extreme response of the system to the perturbations $\mathbf{\Psi}$. This is due to the exacerbated sensitivity of these manifolds to the perturbation of the system. Indeed, as Fig. 11 suggests, the trajectories responsible for these extreme responses concentrate near some heteroclinic connection between the two regimes mentioned in the introduction of Section 3 and depicted in Fig. 2. We see two possibilities to overcome this issue in the case where a long lead-time correction is needed.

– First, as suggested by Eyink et al. (2004), the problem should be studied in other systems. It might be resolved by itself in other systems. Indeed, in very large atmospheric systems, the encounter of such manifolds might become more rare. This could be related to the chaotic hypothesis (Gallavotti and Cohen, 1995a, b) which states that large systems can be considered to behave like Axiom-a hyperbolic systems for the physical quantities of interest, and thus Ruelle response theory (Ruelle, 2009) might get better as the dimensionality of a system increases. This hypothesis would be interesting to test in current state-of-the-art NWP systems.

– Secondly, another avenue would be to adapt the very effective techniques based on the Covariant Lyapunov vectors (CLVs) to non-stationary dynamics. These techniques were recently introduced (Wang, 2013; Ni and Wang, 2017; Ni, 2019) to deal with stationary responses of chaotic systems, i.e. the response of a system that lies on its attractor.

The CLVs methods mentioned focus on finding an adjoint representation (Eyink et al., 2004) of the response, while in the present work the approach is based on forward integrations (direct method). The adjoint representation allows to change easily the perturbation function $\mathbf{\Psi}$ for a fixed observable A, while the direct method allows for different observables to be considered,
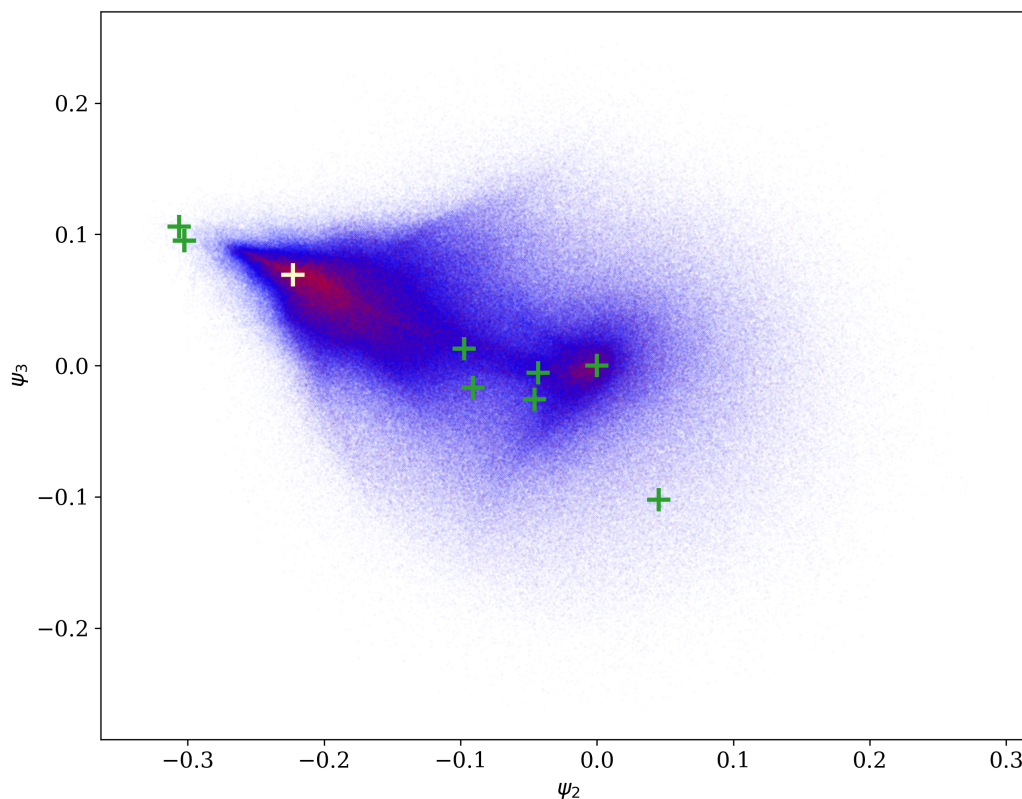
Figure 11. 2D scatter plot showing the phase-space locations of the perturbations composing the fat tails shown in Fig. 9. Blue dots: plot of the trajectories of the model 0 used to compute the average response, along the variables ψ_2 and ψ_3. Red dots: plot of the forecast trajectories of the model 0 leading to an extreme response $\delta\theta_1$ with an absolute deviation from the mean response greater than 100 standard deviations of the distribution shown in Fig. 9. Green crosses: Equilibrium points of model 0. White cross: Location of the maximum perturbation encountered in the data, across all the trajectories and lead times.

while keeping the perturbation function fixed. The adjoint representation, however, requires one to integrate the tangent model backward in time. Therefore, its accuracy depends on the absolute value of the smallest Lyapunov exponent of the system, which might render its results less good than the direct forward representation.

In conclusion, the response-theory approach developed here is an effective method to deal with the problem of the impact of model change on the post-processing scheme. Its main advantage is to be computed on the past model version and does not require reforecasts of the full model. Its operational implementation, however, is still an open question that should be addressed in the future.

Code availability. The quasi-geostrophic model was obtained by adapting the Python code of the MAOOAM ocean-atmosphere model (De Cruz et al., 2016), following the model description in Cehelsky and Tung (1987). The release of the full source code as well as the notebooks generating the figures is in preparation. It will be ready by the end of the discussion process. It will be published on GitHub, and a link will be provided through the Zenodo service.

5 **Appendix A: Non-stationary response theory**

We consider a perturbed autonomous dynamical system

$$\dot{\boldsymbol{y}} = \boldsymbol{F}(\hat{\boldsymbol{y}}) + \boldsymbol{\Psi}(\hat{\boldsymbol{y}}) = \hat{\boldsymbol{F}}(\hat{\boldsymbol{y}}) \tag{A1}$$

with a prescribed distribution of initial conditions ρ_0. For the unperturbed system

$$\dot{\boldsymbol{y}} = \boldsymbol{F}(\boldsymbol{y}), \tag{A2}$$

10 an observable A has the average at time τ

$$\langle A(\tau) \rangle_{\boldsymbol{y}} = \int \mathrm{d}\boldsymbol{y}_0 \, \rho_0(\boldsymbol{y}_0) \, A(\boldsymbol{f}^\tau(\boldsymbol{y}_0)) = \int \mathrm{d}\boldsymbol{y} \, \rho_\tau(\boldsymbol{y}) \, A(\boldsymbol{y}) \tag{A3}$$

where $\boldsymbol{f}^\tau$ is the flow of the unperturbed system (A2) and where ρ_τ is the distribution obtained by propagating the initial distribution ρ_0 with the Liouville equation (Gaspard, 2005). In this section, the variation of this average due to the presence of the perturbation is evaluated,

15 $$\langle A(\tau) \rangle_{\hat{\boldsymbol{y}}} = \langle A(\tau) \rangle_{\boldsymbol{y}} + \delta \langle A(\tau) \rangle_{\boldsymbol{y}} + \delta^2 \langle A(\tau) \rangle_{\boldsymbol{y}} + \dots \tag{A4}$$

In other words, we compute the average of A in system (A1)

$$\langle A(\tau) \rangle_{\hat{\boldsymbol{y}}} = \int \mathrm{d}\boldsymbol{y}_0 \, \rho_0(\boldsymbol{y}_0) \, A(\hat{\boldsymbol{f}}^\tau(\boldsymbol{y}_0)) \tag{A5}$$

as a perturbation of the average (A3) in the unperturbed system (A2). Here, $\hat{\boldsymbol{f}}^\tau$ is the flow of the perturbed system (A1). In the following, we will derive these corrections thanks to a Kubo-type perturbative expansion (Lucarini, 2008) that amounts

20 to constructing a Dyson series in the interaction picture framework where the perturbation is seen as an interaction Hamiltonian (Wouters and Lucarini, 2012). We start by considering the time evolution of the observable A in the system (A1):

$$\frac{\mathrm{d}}{\mathrm{d}\tau} A\left(\hat{\boldsymbol{f}}^\tau(\boldsymbol{y}_0)\right) = (\mathcal{L}_0 + \mathcal{L}_1) \, A\left(\hat{\boldsymbol{f}}^\tau(\boldsymbol{y}_0)\right) \tag{A6}$$

with the operators

25 $$\begin{cases} \mathcal{L}_0 \, A(\boldsymbol{y}) &= \boldsymbol{F}(\boldsymbol{y})^\mathsf{T} \cdot \boldsymbol{\nabla}_{\boldsymbol{y}} A \\ \mathcal{L}_1 \, A(\boldsymbol{y}) &= \boldsymbol{\Psi}(\boldsymbol{y})^\mathsf{T} \cdot \boldsymbol{\nabla}_{\boldsymbol{y}} A \end{cases} \tag{A7}$$

and define an interaction observable as

$$A_I(\tau, \boldsymbol{y}_0) = \Pi_0(-\tau) A\left(\hat{\boldsymbol{f}}^\tau(\boldsymbol{y}_0)\right) \tag{A8}$$

with $\Pi_0(\tau) = \exp\left(\mathcal{L}_0 \tau\right)$. It is easy to show that the interaction observable satisfies the differential equation:

$$\frac{\mathrm{d}}{\mathrm{d}\tau} A_I(\tau, \boldsymbol{y}_0) = \mathcal{L}_I(\tau) A_I(\tau, \boldsymbol{y}_0) \tag{A9}$$

5   with the interaction operator $\mathcal{L}_I(\tau) = \Pi_0(-\tau)\mathcal{L}_1\Pi_0(\tau)$. The solution to this equation is

$$A_I(\tau, \boldsymbol{y}_0) = A_I(0, \boldsymbol{y}_0) + \int_0^\tau \mathrm{d}s_1\, \mathcal{L}_I(s_1) A_I(s_1, \boldsymbol{y}_0) = A(\boldsymbol{y}_0) + \int_0^\tau \mathrm{d}s_1\, \mathcal{L}_I(s_1) A_I(s_1, \boldsymbol{y}_0) \tag{A10}$$

which can be rewritten as

$$A\left(\hat{\boldsymbol{f}}^\tau(\boldsymbol{y}_0)\right) = \Pi_0(\tau) A(\boldsymbol{y}_0) + \int_0^\tau \mathrm{d}s_1\, \Pi_0(\tau - s_1)\mathcal{L}_1\Pi_0(s_1) A_I(s_1, \boldsymbol{y}_0) \quad . \tag{A11}$$

Iteratively replacing the interaction observable by the formula (A10) finally leads to the Dyson series:

$$
\begin{aligned}
10 \quad A\left(\hat{\boldsymbol{f}}^\tau(\boldsymbol{y}_0)\right) &= \Pi_0(\tau) A(\boldsymbol{y}_0) + \int_0^\tau \mathrm{d}s_1\, \Pi_0(\tau - s_1)\mathcal{L}_1\Pi_0(s_1) A(\boldsymbol{y}_0) \\
&\quad + \int_0^\tau \mathrm{d}s_1 \int_0^{s_1} \mathrm{d}s_2\, \Pi_0(\tau - s_1)\mathcal{L}_1\Pi_0(s_1 - s_2)\mathcal{L}_1\Pi_0(s_2) A(\boldsymbol{y}_0) + \dots
\end{aligned}
\tag{A12}
$$

Using the definitions (A3) and (A5), as well as the fact that

$$g\left(\boldsymbol{f}^\tau(\boldsymbol{y}_0)\right) = \Pi_0(\tau) g(\boldsymbol{y}_0) \tag{A13}$$

for any smooth function g, we get finally a formula for the perturbations in Eq. (A4):

$$
15 \quad \langle A(\tau)\rangle_{\hat{\boldsymbol{y}}} = \langle A(\tau)\rangle_{\boldsymbol{y}} + \int_0^\tau \mathrm{d}s_1 \int \mathrm{d}\boldsymbol{y}_0\, \rho_0(\boldsymbol{y}_0)\Pi_0(\tau - s_1)\mathcal{L}_1\Pi_0(s_1) A(\boldsymbol{y}_0) + \dots \tag{A14}
$$

We will now focus on the first term of this expansion, but the subsequent orders of the response can be treated alike. We thus have

$$\delta\langle A(\tau)\rangle_{\boldsymbol{y}} = \int_0^\tau \mathrm{d}s_1 \int \mathrm{d}\boldsymbol{y}_0\, \rho_0(\boldsymbol{y}_0)\,\boldsymbol{\Psi}\left(\boldsymbol{f}^{\tau - s_1}(\boldsymbol{y}_0)\right)^\mathsf{T} \cdot \boldsymbol{\nabla}_{\boldsymbol{f}^{\tau - s_1}(\boldsymbol{y}_0)} A\left(\boldsymbol{f}^\tau(\boldsymbol{y}_0)\right) \tag{A15}$$

which with the change of variable $s_1 \to t - \tau'$ can be rewritten as

$$
20 \quad \delta\langle A(\tau)\rangle_{\boldsymbol{y}} = \int_0^\tau \mathrm{d}\tau' \int \mathrm{d}\boldsymbol{y}_0\, \rho_0(\boldsymbol{y}_0)\,\boldsymbol{\Psi}\left(\boldsymbol{f}^{\tau'}(\boldsymbol{y}_0)\right)^\mathsf{T} \cdot \boldsymbol{\nabla}_{\boldsymbol{f}^{\tau'}(\boldsymbol{y}_0)} A\left(\boldsymbol{f}^\tau(\boldsymbol{y}_0)\right) \tag{A16}
$$

and then

$$\delta\langle A(\tau)\rangle_{\boldsymbol{y}} \quad = \quad \int\limits_0^\tau \mathrm{d}\tau' \int \mathrm{d}\boldsymbol{y}_0\, \rho_0(\boldsymbol{y}_0)\, \boldsymbol{\Psi}\left(\boldsymbol{f}^{\tau'}(\boldsymbol{y}_0)\right)^{\mathsf{T}} \cdot \left(\frac{\partial \boldsymbol{f}^\tau(\boldsymbol{y}_0)}{\partial \boldsymbol{f}^{\tau'}(\boldsymbol{y}_0)}\right)^{\mathsf{T}} \cdot \boldsymbol{\nabla}_{\boldsymbol{f}^\tau(\boldsymbol{y}_0)} A \tag{A17}$$

$$= \quad \int\limits_0^\tau \mathrm{d}\tau' \int \mathrm{d}\boldsymbol{y}_0\, \rho_0(\boldsymbol{y}_0)\, \boldsymbol{\Psi}\left(\boldsymbol{f}^{\tau'}(\boldsymbol{y}_0)\right)^{\mathsf{T}} \cdot \mathbf{M}\left(\tau - \tau', \boldsymbol{f}^{\tau'}(\boldsymbol{y}_0)\right)^{\mathsf{T}} \cdot \boldsymbol{\nabla}_{\boldsymbol{f}^\tau(\boldsymbol{y}_0)} A \tag{A18}$$

$\mathbf{M}$ is the fundamental matrix (Gaspard, 2005; Nicolis, 2016) of the homogeneous part of the linear differential equation

$$\dot{\boldsymbol{\delta y}} = \boldsymbol{\nabla}_{\boldsymbol{y}} \boldsymbol{F} \cdot \boldsymbol{\delta y} + \boldsymbol{\Psi}(\boldsymbol{y}) \tag{A19}$$

where $\boldsymbol{y}$ is solution of Eq. (A2) with initial condition $\boldsymbol{y_0}$, and we have the definition

$$\mathbf{M}(t, \boldsymbol{y}) = \frac{\partial \boldsymbol{f}^t(\boldsymbol{y})}{\partial \boldsymbol{y}} \qquad . \tag{A20}$$

Equation (A19) is the linearised approximation of equation (A1):

$$\dot{\boldsymbol{y}} + \dot{\boldsymbol{\delta y}} = \boldsymbol{F}(\boldsymbol{y} + \boldsymbol{\delta y}) + \boldsymbol{\Psi}(\boldsymbol{y} + \boldsymbol{\delta y}) \tag{A21}$$

that provides a tool to estimate Eq. (A18). Indeed, since the solution of Eq. (A19) can be written as

$$\boldsymbol{\delta y}(\tau) = \int\limits_0^\tau \mathrm{d}\tau'\, \mathbf{M}\left(\tau - \tau', \boldsymbol{f}^{\tau'}(\boldsymbol{y_0})\right) \cdot \boldsymbol{\Psi}\left(\boldsymbol{f}^{\tau'}(\boldsymbol{y_0})\right) \quad , \tag{A22}$$

we can write the first order variation of the average of the observable A in term of these solutions:

$$\delta\langle A(\tau)\rangle_{\boldsymbol{y}} = \int \mathrm{d}\boldsymbol{y}_0\, \rho_0(\boldsymbol{y}_0)\, \boldsymbol{\delta y}(\tau)^{\mathsf{T}} \cdot \boldsymbol{\nabla}_{\boldsymbol{f}^\tau(\boldsymbol{y}_0)} A \tag{A23}$$

The interpretation of this equation is that the averaging of an observable over the trajectories of the linear approximation (A21) of the perturbation equation (A1) provides the first order response of the observable. It is the main ingredient used to compute the new post-processing scheme in the present work. It is explained in detail in Sections 2.3 and 3.2.

Competing interests. Stéphane Vannitsem is a member of the editorial board of the journal. Jonathan Demaeyer declares that he has no conflict of interest.

Acknowledgements. This work is supported in part by the Post-Processing module of the NWP Cooperation program of the European Meteorological Network (EUMETNET). The authors warmly thank Lesley De Cruz for her suggestions throughout the manuscript.

References

Bonavita, M., Trémolet, Y., Holm, E., Lang, S. T., Chrust, M., Janisková, M., Lopez, P., Laloyaux, P., De Rosnay, P., Fisher, M., et al.: A strategy for data assimilation, European Centre for Medium Range Weather Forecasts, 2017.

Cehelsky, P. and Tung, K. K.: Theories of multiple equilibria and weather regimes—A critical reexamination. Part II: Baroclinic two-layer models, Journal of the atmospheric sciences, 44, 3282–3303, 1987.

Charney, J. G. and Straus, D. M.: Form-drag instability, multiple equilibria and propagating planetary waves in baroclinic, orographically forced, planetary wave systems, Journal of the Atmospheric Sciences, 37, 1157–1176, 1980.

De Cruz, L., Demaeyer, J., and Vannitsem, S.: The Modular Arbitrary-Order Ocean-Atmosphere Model: MAOOAM v1.0, Geoscientific Model Development, 9, 2793–2808, 2016.

Eyink, G., Haine, T., and Lea, D.: Ruelle's linear response formula, ensemble adjoint schemes and Lévy flights, Nonlinearity, 17, 1867, 2004.

Gallavotti, G. and Cohen, E.: Dynamical ensembles in nonequilibrium statistical mechanics, Physical Review Letters, 74, 2694, 1995a.

Gallavotti, G. and Cohen, E. G. D.: Dynamical ensembles in stationary states, Journal of Statistical Physics, 80, 931–970, 1995b.

Gardiner, C. W.: Handbook of stochastic methods, Springer Berlin, fourth edn., 2009.

Gaspard, P.: Chaos, scattering and statistical mechanics, vol. 9, Cambridge University Press, 2005.

Glahn, B., Peroutka, M., Wiedenfeld, J., Wagner, J., Zylstra, G., Schuknecht, B., and Jackson, B.: MOS uncertainty estimates in an ensemble framework, Monthly Weather Review, 137, 246–268, 2009.

Glahn, H. R. and Lowry, D. A.: The use of model output statistics (MOS) in objective weather forecasting, Journal of applied meteorology, 11, 1203–1211, 1972.

Gottwald, G. A., Wormell, J., and Wouters, J.: On spurious detection of linear response and misuse of the fluctuation–dissipation theorem in finite time series, Physica D: Nonlinear Phenomena, 331, 89–101, 2016.

Hagedorn, R., Hamill, T. M., and Whitaker, J. S.: Probabilistic forecast calibration using ECMWF and GFS ensemble reforecasts. Part I: Two-meter temperatures, Monthly Weather Review, 136, 2608–2619, 2008.

Hamill, T. M.: Practical aspects of statistical postprocessing, in: Statistical Postprocessing of Ensemble Forecasts, edited by Vannitsem, S., Wilks, D. S., and Messner, J. W., pp. 187–217, Elsevier, 2018.

Hamill, T. M., Hagedorn, R., and Whitaker, J. S.: Probabilistic forecast calibration using ECMWF and GFS ensemble reforecasts. Part II: Precipitation, Monthly weather review, 136, 2620–2632, 2008.

Hamill, T. M., Bates, G. T., Whitaker, J. S., Murray, D. R., Fiorino, M., Galarneau Jr, T. J., Zhu, Y., and Lapenta, W.: NOAA's second-generation global medium-range ensemble reforecast dataset, Bulletin of the American Meteorological Society, 94, 1553–1565, 2013.

Johnson, C. and Bowler, N.: On the reliability and calibration of ensemble forecasts, Monthly Weather Review, 137, 1717–1720, 2009.

Lang, M. N., Lerch, S., Mayr, G. J., Simon, T., Stauffer, R., and Zeileis, A.: Remember the past: A comparison of time-adaptive training schemes for non-homogeneous regression, Nonlinear Processes in Geophysics Discussions, 2019, 1–18, 2019.

Lucarini, V.: Response theory for equilibrium and non-equilibrium statistical mechanics: Causality and generalized Kramers-Kronig relations, Journal of Statistical Physics, 131, 543–558, 2008.

Lucarini, V.: Stochastic perturbations to dynamical systems: a response theory approach, Journal of Statistical Physics, 146, 774–786, 2012.

Ni, A.: Hyperbolicity, shadowing directions and sensitivity analysis of a turbulent three-dimensional flow, Journal of Fluid Mechanics, 863, 644–669, 2019.

Ni, A. and Wang, Q.: Sensitivity analysis on chaotic dynamical systems by Non-Intrusive Least Squares Shadowing (NILSS), Journal of Computational Physics, 347, 56–77, 2017.

Nicolis, C.: Dynamics of model error: Some generic features, Journal of the Atmospheric Sciences, 60, 2208–2218, 2003.

Nicolis, C.: Error dynamics in extended-range forecasts, Quarterly Journal of the Royal Meteorological Society, 142, 1222–1231, 2016.

5 Reinhold, B. B. and Pierrehumbert, R. T.: Dynamics of weather regimes: Quasi-stationary waves and blocking, Monthly Weather Review, 110, 1105–1145, 1982.

Ruelle, D.: General linear response formula in statistical mechanics, and the fluctuation-dissipation theorem far from equilibrium, Physics Letters A, 245, 220–224, 1998a.

Ruelle, D.: Nonequilibrium statistical mechanics near equilibrium: computing higher-order terms, Nonlinearity, 11, 5, 1998b.

10 Ruelle, D.: A review of linear response theory for general differentiable dynamical systems, Nonlinearity, 22, 855, 2009.

Scheuerer, M. and Hamill, T. M.: Statistical postprocessing of ensemble precipitation forecasts by fitting censored, shifted gamma distributions, Monthly Weather Review, 143, 4578–4596, 2015.

Van Schaeybroeck, B. and Vannitsem, S.: Ensemble post-processing using member-by-member approaches: theoretical aspects, Quarterly Journal of the Royal Meteorological Society, 141, 807–818, 2015.

15 Vannitsem, S.: A unified linear model output statistics scheme for both deterministic and ensemble forecasts, Quarterly Journal of the Royal Meteorological Society, 135, 1801–1815, 2009.

Vannitsem, S.: Bias correction and post-processing under climate change, Nonlinear Processes in Geophysics, 18, 911–924, 2011.

Vannitsem, S.: Predictability of large-scale atmospheric motions: Lyapunov exponents and error dynamics, Chaos: An Interdisciplinary Journal of Nonlinear Science, 27, 032 101, 2017.

20 Vannitsem, S. and Nicolis, C.: Dynamical properties of model output statistics forecasts, Monthly Weather Review, 136, 405–419, 2008.

Vannitsem, S., Wilks, D. S., and Messner, J.: Statistical postprocessing of ensemble forecasts, Elsevier, 2018.

Wang, Q.: Forward and adjoint sensitivity computation of chaotic dynamical systems, Journal of Computational Physics, 235, 1–13, 2013.

Wilks, D. S.: Statistical methods in the atmospheric sciences, vol. 100, Academic press, 2011.

Wormell, C. L. and Gottwald, G. A.: On the validity of linear response theory in high-dimensional deterministic dynamical systems, Journal

25 of Statistical Physics, 172, 1479–1498, 2018.

Wouters, J. and Lucarini, V.: Disentangling multi-level systems: averaging, correlations and memory, Journal of Statistical Mechanics: Theory and Experiment, 2012, P03 003, 2012.